THE JOURNAL OF PHYSICAL CHEMISTRY B

ARTICLE

pubs.acs.org/JPCB

Liquid Structure of and Li^+ Ion Solvation in Bis(trifluoromethanesulfonyl)amide Based Ionic Liquids Composed of 1-Ethyl-3-methylimidazolium and *N*-Methyl-*N*-propylpyrrolidinium Cations

Yasuhiro Umebayashi,[*,†] Hiroshi Hamano,[†] Shiro Seki,[§] Babak Minofar,[†] Kenta Fujii,[‡] Kikuko Hayamizu,[∥] Seiji Tsuzuki,[∥] Yasuo Kameda,[⊥] Shinji Kohara,[#] and Masayoshi Watanabe[▽]

[†] Department of Chemistry, Faculty of Science, Kyushu University, Hakozaki, Higashi-ku, Fukuoka 812-8581, Japan

[‡] Neutron Scattering Laboratory, Institute for Solid State Physics, The University of Tokyo, Kashiwa, Chiba 277-8581, Japan

[§] Materials Science Research Laboratory, Central Research Institute of Electric Power Industry (CRIEPI), 2-11-1, Iwado-kita, Komae, Tokyo 201-8511, Japan

[∥] National Institute of Advanced Industrial Science and Technology (AIST), Tsukuba Center, Tsukuba, Ibaraki, 305-8565, Japan

[⊥] Department of Material and Biological Chemistry, Faculty of Science, Yamagata University, 1-4-12 Kojirakawa-machi, Yamagata 990-8560, Japan

[#] Japan Synchrotron Radiation Research Institute (JASRI), Sayo-cho, Sayo-gun, Hyogo 679-5198, Japan

[▽] Department of Chemistry and Biotechnology, Yokohama National University, 79-5 Tokiwadai Hodogaya-ku, Yokohama 240-8501, Japan

Supporting Information

ABSTRACT: Liquid structures of the bis(trifluoromethanesulfonyl)amide based ionic liquids composed of 1-ethyl-3-methylimidazolium and *N*-methyl-*N*-propylpyrrolidinium ($[C_2mIm^+][TFSA^-]$ and $[C_3mPyrro^+][TFSA^-]$, respectively) and Li^+ ion solvation structure in their lithium salt solutions were studied by means of high-energy X-ray diffraction (HEXRD) technique with the aid of MD simulations. With regard to neat ionic liquids, a small but significant difference was found at around 3.5 Å in the intermolecular radial distribution functions $G_{inter}(r)$s for these two ionic liquids; i.e., $G_{inter}(r)$ for $[C_2mIm^+][TFSA^-]$ was positioned at a slightly shorter region relative to that for $[C_3mPyrro^+][TFSA^-]$, which suggests that the nearest neighboring cation−anion interaction in the imidazolium ionic liquid is slightly greater than that in the other. With regard to Li^+ ion solvation structure, $G_{inter}(r)$s for $[C_2mIm^+][TFSA^-]$ dissolving Li^+ ion exhibited additional small peak of about 1.9 Å attributable to the Li^+−O ($TFSA^-$) atom−atom correlation, though the corresponding peak was unclear in $[C_3mPyrro^+][TFSA^-]$ due to overlapping with the intramolecular atom−atom correlations in $[C_3mPyrro^+]$. In addition, the long-range density fluctuation observed in the neat ionic liquids diminished with the increase of Li^+ ion concentration for both ionic liquid solutions. These observations indicate that the large scale Li^+ ion solvated clusters are formed in the TFSA based ionic liquids, and well support the formation of $[Li(TFSA)_2]^+$ cluster clarified by previous Raman spectroscopic studies. MD simulations qualitatively agree with the experimental facts, by which the decrease in the long-range oscillation amplitude of $r^2\{G(r) - 1\}$ for the Li^+ containing ionic liquids can be ascribed to the variation in the long-range anion−anion correlations caused by the formation of the Li^+ ion solvated clusters.

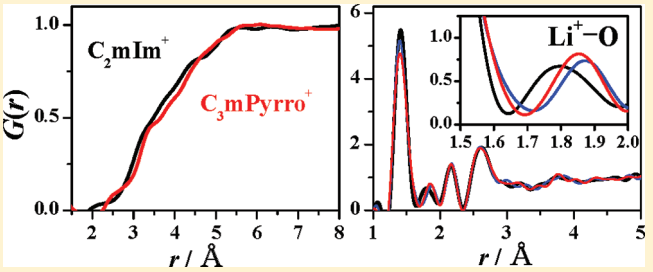

INTRODUCTION

Room-temperature ionic liquids have attracted remarkable attention not only in their application owing to the favorable properties such as negligible vapor pressure, low flammability, and high thermal and electrochemical stability[1,2] but also, from fundamental viewpoints, in solution chemistry and condensed or soft matter sciences.[3−8] Among a wide range of their applications, the lithium secondary batteries are one of the promising ones.[9−13] It is practically important to elucidate the lithium ion conduction mechanism in bulk solution and particularly at the electrolyte solution/electrode interface where the electron transfer is accompanied by the Li^+ ion solvation/desolvation.[14,15]

Received: July 30, 2011
Revised: September 7, 2011
Published: September 30, 2011

From the viewpoint of electrolyte solution chemistry at a molecular level, the structure and dynamics of the lithium ion in the bis(trifluoromethanesulfonyl)amide ($TFSA^-$) based ionic liquids have been much explored until now, for instance, the conformational isomerism of $TFSA^-$;[16−19] followed by the lithium ion solvation structure by means of Raman/IR spectroscopy,[20−24] the self-diffusion coefficient by the pulse gradient spin echo NMR,[25−36] and the collective dynamics by the optical Kerr effect spectroscopy[37] have been reported. Theoretical approaches such as ab initio calculations[38,39] and molecular simulations[40,41] are also useful for this purpose. Apart from ionic liquid solutions, the lithium ion solvation and the ion-paired structures in aqueous and nonaqueous solutions is well investigated by means of neutron/X-ray diffraction techniques.[42−51]

In classical electrolyte solution chemistry, it is well accepted that the Stokes law simply describes the ionic conductivity in solution as a function of the solution viscosity and the "hydrodynamic" ionic radius in solution so-called "Stokes radii"; however, the validity of the Stokes law breaks even for the metal ions such as alkaline metal and alkaline earth metal ions in aqueous solutions. Recent statistical mechanics liquid theory and molecular simulation partially succeeded in explaining the Stokes law breakdown.[52,53] More sophisticated theories were developed for describing the solution viscosity and the ionic conductivity in electrolyte solutions based on the mode coupling theory and the integral equation theory based on the interaction site model,[54−56] in which static and dynamic structure factors play an important role to link macroscopic transport properties of electrolyte solutions with microscopic structural features at a molecular level. Therefore, direct neutron/X-ray scattering measurements are indispensable to yield experimental static and dynamic structure factors for electrolyte solutions of ionic liquids, though numerous crystal structures of ionic liquids have been accumulated and reviewed.[57−59]

We have so far studied the conformational isomerism of $TFSA^-$ and its analogue FSA^- (bis(fluorosulfonyl)amide) anions,[60−64] the lithium ion solvation,[65−68] and the liquid structure of several ionic liquids.[64,69−74] In addition, Raman/IR spectroscopy is suitable to explore the lithium ion solvation in the ionic liquids[25−36,65−68] and the conformational isomerization of solvent anions in bulk and the first coordination shell of the lithium ion in ionic liquids.[17−19,60−64] Moreover, though indirect, it yields information on the Li^+−O ($TFSA^-$) distance in the lithium ion solvated in ionic liquids.[67] More direct information on the bond length, of course, should be evaluated by means of neutron/X-ray diffraction techniques. However, it is not easy to clarify even the liquid structure of neat ionic liquids themselves due to the large molecular size and the flexibility of the composing ions, and thus the quite complicated atom−atom correlations involved in the system. In fact, at the present stage, the difference between the imidazolium and the pyrrolidinium based ionic liquids in the structural aspect of the closest cation−anion interaction is unclear, and also the bond length of the Li^+−O ($TFSA^-$) in the solvated lithium ion. Furthermore, it should be noted that, in general, X-ray diffraction is not suitable to explore the lithium ion solvation structure in solution because its number of electrons is only two.

On the other hand, to achieve high real-space resolution in the X-ray diffraction experiments, high-energy X-ray obtained by synchrotron radiation is rather useful. In this work, we demonstrate that the high-energy X-ray diffraction technique (HEXRD) with the aid of molecular dynamics simulations can reveal rather small structural differences in terms of the closest ion−ion interaction between 1-ethyl-3-methylimidazolium [C_2mIm^+] and *N*-methyl-*N*-propylpyrrolidinium [$C_3mPyrro^+$] based ionic liquids coupled with $TFSA^-$, and though, qualitatively, high-real space resolution of HEXRD can yield information on the Li^+−O ($TFSA^-$) bond length in the lithium ion solvated cluster in the $TFSA^-$ based ionic liquids. We also describe our finding that the dissolution of the lithium ion into the ionic liquids gives significant variations in the long-range density fluctuation of the neat ionic liquids because of the formation of the large scale lithium ion solvated clusters.

EXPERIMENTAL SECTION

Materials. [C_2mIm^+][$TFSA^-$] and [$C_3mPyrro^+$][$TFSA^-$] ionic liquids were synthesized according to the ordinary method.[75−77] Water content was checked by a Karl Fischer coulombmetric titration to be less than 20 ppm, and a halide ion presence was checked by an $AgNO_3$ test to be negligible. LiTFSA salt (Morita Chemical Industries Co. Ltd.) was dried in vacuo at 425 K for 1 day and used without further purification. All materials were treated and stored in a high performance glovebox equipped with moisture and oxygen sensors (MIWA MFG Co. Ltd.), in which water and oxygen contents were kept less than 1 ppm.

HEXRD Experiments. HEXRD measurements were carried out at 298 K using the BL04B2 beamline of SPring-8 at the Japan Synchrotron Radiation Research Institute (JASRI).[78,79] Sample ionic liquid was set in a cell consisting of a 2 mm thick polyetheretherketone plate as a body with Kapton films as an X-ray window hermetically sealed with Kalrez O rings, and stainless steel cover plates. Monochrome 61.6 keV X-rays were obtained using a Si(220) monochromator. For the HEXRD measurement of ionic liquid samples, 6−8 h of X-ray irradiation was needed to achieve enough *S*/*N*. In our own experience, there is no sample damage by such high-energy X-ray irradiation. The observed X-ray intensity was corrected for absorption[80] and polarization. Incoherent scatterings[81−83] were subtracted to obtain coherent scatterings, $I_{coh}(Q)$. The X-ray structure factor $S^{HEXRD}(Q)$ and X-ray radial distribution function $G^{HEXRD}(r)$ per stoichiometric volume were respectively obtained according to

$$S^{HEXRD}(Q) = \frac{I_{coh}(Q) - \sum n_i f_i(Q)^2}{(\sum n_i f_i(Q))^2} + 1 \quad (1)$$

$$G^{HEXRD}(r) - 1 = \frac{1}{2\pi^2 r \rho_0} \int_0^{Q_{max}} Q\{S(Q) - 1\} \sin(Qr) \exp(-BQ^2)\, dQ \quad (2)$$

where n_i and $f_i(Q)$ denote the number and atomic scattering factor of atom *i*,[84] respectively, ρ_0 is the number density, and *B* is the damping factor. All data treatment was carried out using the program KURVLR.[85]

MD Simulations. All MD simulations in this study are based on the OPLS-AA manner[86,87] except combination rules; Lorentz−Berthelot rules (arithmetic and geometric mean for σ and ε, respectively). CLaP force fields[88−92] were used for the neat ionic liquids in this study to keep consistency comparing ionic liquids consisting of two different cations, though some reviews were published,[93,94] and new force fields[95−101] and a many body polarizable model[102−111] have been recently developed for the imidazolium and the pyrrolidinium based ionic liquids, which successfully described the structure and dynamics of these ionic

liquids. LJ parameters proposed by Soetens et al. for the lithium ion in nonaqueous cyclic/acyclic carbonate solutions were employed.[112] New sets for the lithium ion in an aqueous solution have been proposed by Joung et al. based on the hydration free energy.[113] These two sets of LJ parameters are surprisingly similar and practically the same with each other. In fact, we calculated the same system using the latter parameters to confirm both force fields gave practically the same results.

In our simulations, Gear's predictor-corrector algorithm[114,115] was employed for integration of the equations of motion with 0.2 fs time steps. The systems contained 256 ion pairs under *NTP* ensemble conditions controlled by the Nose thermostat[116,117] and the Parrinello−Rahman barostat.[118,119] The latter was always set to atmospheric pressure. Long-range interactions were estimated using the Ewald summation method with real-space cutoff distances of 11 Å. The simulation runs typically consisted of 2.5−3.5 ns equilibration periods followed by 0.5 ns production runs, whose trajectories were then analyzed. All simulations were carried out using a Fujitsu Materials Explorer 4.0 program suite on the Fujitsu PRIMEQUEST 580 at the Computing and Communications Center, Kyushu University.The X-ray structure factor $S^{MD}(Q)$ was calculated as

$$\begin{cases} S^{MD}(Q) = \dfrac{\sum_i \sum_j \{n_i(n_j-1)f_i(Q)f_j(Q)/N(N-1)\}}{\{\sum_k (n_k f_k(Q)/N)\}^2} \times \int_0^r 4\pi r^2 \rho_0 (g_{ij}^{MD}(r)-1)\dfrac{\sin(Qr)}{Qr}\,dr + 1 \quad (i=j) \\ S^{MD}(Q) = \dfrac{\sum_i \sum_j (2n_i n_j f_i(Q)f_j(Q)/N^2)}{\{\sum_k (n_k f_k(Q)/N)\}^2} \times \int_0^r 4\pi r^2 \rho_0 (g_{ij}^{MD}(r)-1)\dfrac{\sin(Qr)}{Qr}\,dr + 1 \quad (i \neq j) \end{cases} \tag{3}$$

where ρ_0 denotes the ensemble average of the number density and the total number of atoms in the simulation box N is given by

$$N = \sum_k n_k \tag{4}$$

The X-ray radial distribution function $G^{MD}(r)$ was obtained from $S^{MD}(Q)$ by a Fourier transform procedure similar to that of $S^{HEXRD}(Q)$.

RESULTS AND DISCUSSION

The Closest Cation−Anion Interaction in the Neat Ionic Liquids. Observed X-ray structure factors $S^{HEXRD}(Q)$ at the Q-range of $0 < Q/Å^{-1} < 2.5$ for $[C_2mIm^+][TFSA^-]$ and $[C_3mPyrro^+][TFSA^-]$ were shown in Figure 1a and b, respectively. Those at the full Q-range examined ($Q < 25$ Å^{-1}) were also shown in Figure S1 (given as Supporting Information). Comparing with $S^{HEXRD}(Q)$ for $[C_3mPyrro^+][TFSA^-]$ with that previously reported for $[C_3mPyrro^+][FSA^-]$,[64] a difference can be obviously found in the higher Q-range owing to the intramolecular structures on these anions. Moreover, in the low Q-range of $Q < 2.5$ Å^{-1}, $S^{HEXRD}(Q)$for $[C_3mPyrro^+][TFSA^-]$ was remarkably different from that for $[C_3mPyrro^+][FSA^-]$,

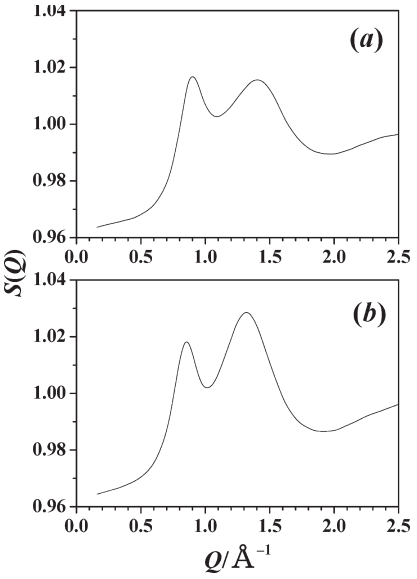

Figure 1. Observed X-ray structure factors at 298 K for $[C_2mIm^+][TFSA^-]$ (upper) and $[C_3mPyrro^+][TFSA^-]$ (lower) neat ionic liquids at the Q range of $0 < Q/Å^{-1} < 2.5$.

suggesting that the intermolecular ion−ion interactions in these ionic liquids are different from each other. The more extensive anion dependence of the liquid structure of ionic liquids will be discussed in detail in our future paper. Both $S^{HEXRD}(Q)$s examined in this study were in accordance with those previously measured by using the ordinary X-ray apparatus with Mo Kα radiation.[69,70] Tiny differences can be found in the high Q-range of $Q > 5$ Å^{-1} mainly due to the intramolecular structure of these cations. Clearly, the high Q-range $S^{HEXRD}(Q)$s for these ionic liquids can be predominantly attributable to the intramolecular structure of $TFSA^-$ of large X-ray scattering ability. On the other hand, a small but significant difference can be found in the low Q-region of $Q < 2.5$ Å^{-1}; i.e., the first and second peaks appeared at 0.90 and 1.42 Å^{-1}, respectively, for $[C_2mIm^+][TFSA^-]$ and the former intensity is higher than the latter, while for $[C_3mPyrro^+][TFSA^-]$ those observed at 0.87 and 1.31 Å^{-1}, and, on the contrary, the second peak was higher in intensity. In addition, the second peak for $[C_2mIm^+][TFSA^-]$ was slightly broader than that for $[C_3mPyrro^+][TFSA^-]$. These observations strongly suggest that the intermolecular atom−atom correlations in $[C_2mIm^+][TFSA^-]$ are positioned more near side relative to those in $[C_3mPyrro^+][TFSA^-]$.

Figure S1 also displays the intramolecular structure factors for the composing ions evaluated by using the following equation:

$$S_{intra}(Q) = \sum (1 + \delta_{ij}) n_{ij} f_i(Q) f_j(Q) \frac{\sin(Qr_{ij})}{Qr_{ij}} \exp(-b_{ij}Q^2) \tag{5}$$

where δ, n_{ij}, and b_{ij} stand for the Kronecker delta, the number of the intramolecular atom−atom pairs, and the temperature factor for atoms i and j, respectively. As already mentioned in the Introduction, the atom−atom correlations included in the closest ion−ion interaction seriously overlap with the relatively far, chemically nonbonded atom−atom correlations involved in the intramolecular geometry of the respective composing ion. In this case, to yield the intermolecular atom−atom correlations

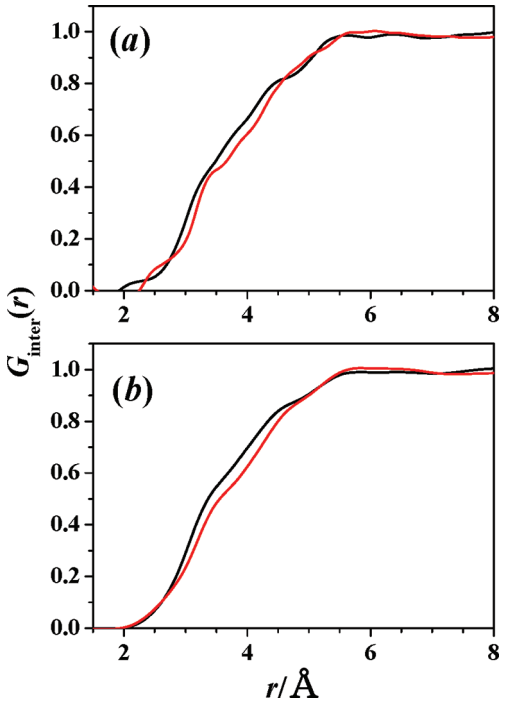

Figure 2. X-ray intermolecular radial distribution functions $G_{inter}(r)$ for $[C_2mIm^+][TFSA^-]$ (black) and $[C_3mPyrro^+][TFSA^-]$ (red), respectively, by means of HEXRD experiments (a) and MD simulations (b), respectively, where the window function is $W(Q) = \exp(-BQ^2)$; $B = 0.011$ was used in both Fourier transformations.

with physical meanings, it is important to evaluate the molecular flexibility accurately and precisely. We have already evaluated thermodynamic quantities for the conformational isomerism of $[C_2mIm^+]$,[120] $[C_3mPyrro^+]$,[121] and $[TFSA^-]$,[60] which are consistent with ab initio calculations and MD simulations.[62,121,122] The intramolecular structure factors were thus estimated according to approximately 1:1 existence of the predominant conformational isomers for the respective ion based on their thermodynamic quantities, i.e., the planar and the nonplanar $[C_2mIm^+]$, the e4 and the e6 $[C_3mPyrro^+]$, and the cis and the trans $[TFSA^-]$.

As can be seen in Figure S1 (Supporting Information), the estimated intramolecular structure factors for both ionic liquids were in good agreement with the observed $S^{HEXRD}(Q)$ at about $Q > 3.5$ Å^{-1}. The intermolecular structure factor $S_{inter}(Q)$ was evaluated according to a simple equation of $S_{inter}(Q) = S(Q) - S_{intra}(Q)$, where $S_{intra}(Q)$ represents the intramolecular structure factor. Thus evaluated $S_{inter}(Q)$s for both neat ionic liquids were shown in Figure S2 (Supporting Information). The intermolecular radial distribution functions (RDFs) $G_{inter}(r)$s were calculated as the Fourier transform of $S_{inter}(Q)$, and given in Figure 2. Similarly total RDF $G(r)$ as the FT of $S(Q)$ was shown in Figure S3 (Supporting Information). As can be shown in Figure S3 (Supporting Information), $G_{intra}(r)$s have significant values still $r < 5$ Å, where they seriously overlapped with the $G_{inter}(r)$. Clearly shown in Figure 2, the $G_{inter}(r)$ for $[C_2mIm^+][TFSA^-]$ located in the shorter r region than that for $[C_3mPyrro^+][TFSA^-]$ to some extent, indicating that some of the atom–atom correlations involved in the nearest neighboring cation–anion interaction in $[C_2mIm^+][TFSA^-]$ are shorter than those in $[C_3mPyrro^+][TFSA^-]$. This observation evidently suggests that the nearest neighboring cation–anion interaction of $[C_2mIm^+]\cdots[TFSA^-]$ is stronger than $[C_3mPyrro^+]\cdots[TFSA^-]$. Though unclear, some shoulders and/or peaks can be found in the respective $G_{inter}(r)$ at about 3.5, 4.0, 4.5, and 5.5 Å. We will discuss such shoulders or peaks with the aid of MD simulations.

The liquid structure of several ionic liquids and their solutions has been published. Here, we briefly survey previously published works by means of neutron/X-ray diffraction experiments for ionic liquids, and discuss our results comparing with them. Neutron diffraction of $[C_2mIm^+][AlCl_4^-]$ has been measured for the first time, and the anionic species were analyzed on the basis of ab initio calculations,[123] recently followed by analyzing with newly developed reverse Monte Carlo technique considering the intramolecular flexibility (RMC-MM).[124] HEXRD experiments for $[C_1Im][F\cdot 2.3HF]$ (C_1Im = 1-methylimidazolium) and $[C_nmIm][F\cdot 2.3HF]$ (n = 2, 4, and 6) have been carried out, and the anionic species were also analyzed.[125,126] Hardacre et al. have extensively reported liquid structures of $[C_1mIm^+][Cl^-]$ and $[C_1mIm^+][PF_6^-]$ (C_1mIm^+; 1-methyl-3-methylimidazolium),[127,128] benzene solutions of $[C_1mIm^+][PF_6^-]$,[129] $[C_1mIm^+][TFSA^-]$,[130] $[C_1PyCN^+][TFSA^-]$[131] and its 1-methylnaphthalene solutions,[132] $[C_2mIm^+][CH_3COO^-]$[133] and $[C_nmIm^+][PF_6^-]$ (n = 4, 6, and 8)[134] by means of neutron diffraction with empirical structure and potential refinement (EPSR) analyses. Kanakubo and Kameda et al. have explored the solvation structure of the CO_2 in its mixtures of $[C_4mIm^+][PF_6^-]$[135] and $[C_4mIm^+][BF_4^-]$[136] with ordinary X-ray diffraction experiments, and the short-range ion–ion interaction in neat $[C_4mIm^+][PF_6^-]$ by means of neutron diffraction with the H/D isotopic substitution technique.[137] Structural similarity between the liquid and the crystal states of $[C_4mIm^+][I^-]$ has been discussed based on the X-ray diffraction experiments.[138] After our publications,[64,69−74] several research groups have reported static X-ray structure factors for ionic liquids explored with combined techniques of X-ray scattering experiments and MD simulations by Caminiti and Triolo et al.,[139−141] the Castner and Margulis groups,[142−144] and the Saboungi group.[145,146] Thus, many liquid structure data of ionic liquids have been accumulated until now. However, most of them focused on the imidazolium based ionic liquids. To the best of our knowledge, the aforementioned fairly small structural difference found in $S^{HEXRD}(Q)$ due to the cation species has never been discussed at the present stage.

Figure S2 (Supporting Information) and Figure 2b also show the intermolecular X-ray structure factors $S^{MD}_{inter}(Q)$s and the intermolecular X-ray radial distribution functions $G^{MD}_{inter}(r)$s calculated from MD simulations for both neat ionic liquids. As can be seen in both figures, MD simulations agreed well with those observed ones by the HEXRD experiments. Before a detailed discussion, it is worth mentioning center-of-mass pair correlation functions evaluated from MD simulations, as shown in Figure 3. Although MD simulations for $[C_2mIm^+][TFSA^-]$ and $[C_3mPyrro^+][TFSA^-]$ have been published by many research groups, center-of-mass pair correlation functions have been scarcely reported.[102,110,147] Our center-of-mass pair correlation functions are consistent with those previously published. The first peak appeared at 4.9 Å with a shoulder of 5.8 Å in the cation–anion RDF for $[C_2mIm^+][TFSA^-]$, while that found at 5.3 Å with a shoulder of 6.5 Å for $[C_3mPyrro^+][TFSA^-]$, which obviously indicates that the closest ion–ion interaction of $[C_2mIm^+]\cdots[TFSA^-]$ is stronger than $[C_3mPyrro^+]\cdots[TFSA^-]$, and well supports the experimental facts.

Figure 4 displays partial atom−atom pair correlation functions of C*n*−O (TFSA) $g_{Cn-O}(r)$s and C*n*−F (TFSA) $g_{Cn-F}(r)$s for both neat ionic liquids (C*n* stands for the respective carbon atom involving each cation, see Chart 1), which are in good agreement with those previously reported.[69,70,147] For both ionic liquids, the peaks of 3.5, 4.0, 4.5, and 5.5 Å in $g_{Cn-O}(r)$s and $g_{Cn-F}(r)$s can clearly be noticed, which are consistent with those observed experimentally. The first peaks appearing in the $g_{Cn-O}(r)$s were higher in intensity than the corresponding $g_{Cn-F}(r)$s except the C9 of [C_3mPyrro$^+$][TFSA$^-$]. Clearly, both cations prefer the oxygen atoms of TFSA$^-$ anion as an interaction site to the fluorine. TFSA$^-$ oxygen prefers the carbons of [C_2mIm$^+$] in the order of C6 ≫ C2 > C4, C7 and C8 > C5, while they populated near [C_3mPyrro$^+$] with C6 > C2 and C5 > C3 and C4, and C7 > C8 and C9. In both izonic liquids, the *N*-methyl group attracts the TFSA$^-$ oxygens most largely in population probably due to

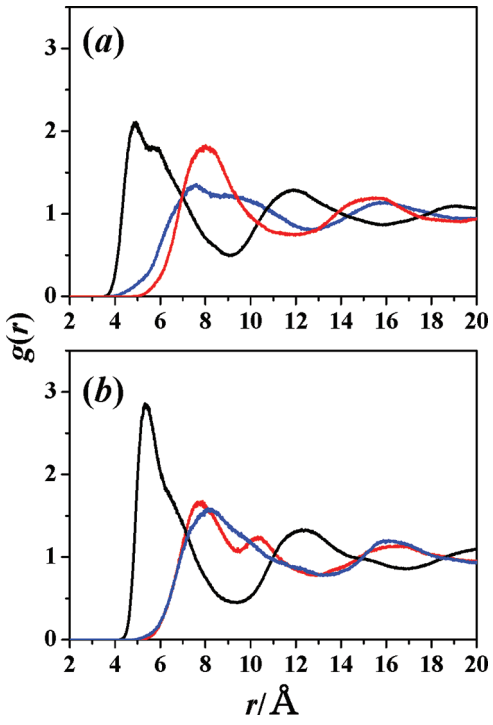

Figure 3. Center-of-mass pair correlation functions for cation−anion (black), cation−cation (blue), and anion−anion (red) derived from MD simulations for [C_2mIm$^+$][TFSA$^-$] (a) and [C_3mPyrro$^+$][TFSA$^-$] (b), respectively.

Chart 1. Schematic Illustration of Molecular Structures of 1-Ethyl-3-methylimidazolium [C_2mIm$^+$], *N*-Methyl-*N*-propylpyrrolidinium [C_3mPyrro$^+$], and Bis(trifluoromethanesulfonyl)amide [TFSA$^-$]

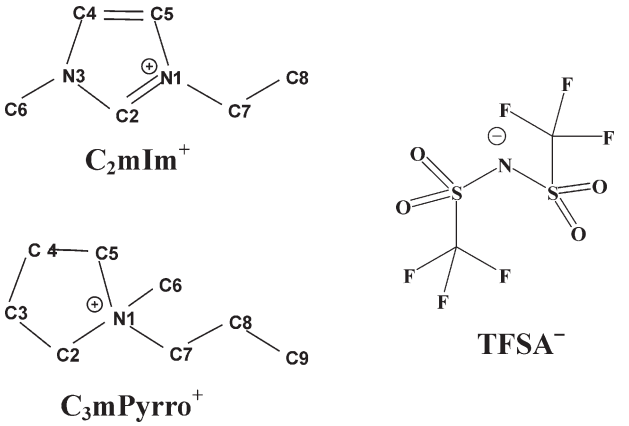

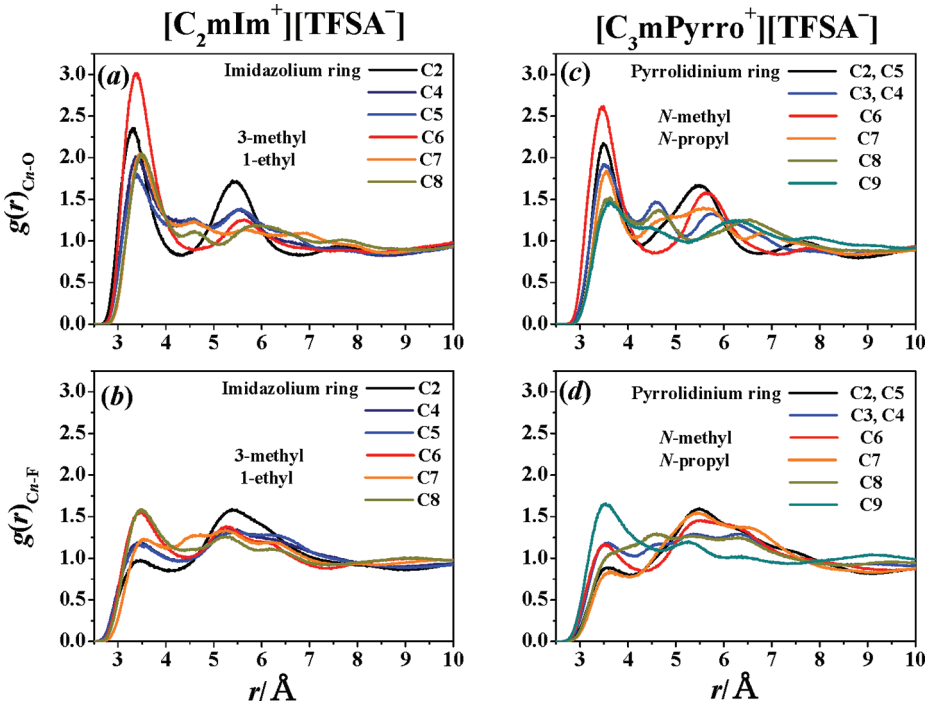

Figure 4. Atom−atom pair correlation functions of C*n*−O and C*n*−F derived from MD simulations for [C_2mIm$^+$][TFSA$^-$] (a and b) and [C_3mPyrro$^+$][TFSA$^-$] (c and d), respectively.

dx.doi.org/10.1021/jp2072827 |*J. Phys. Chem. B* 2011, 115, 12179–12191

their spatial availability. It should be noted that the first peak position in $g_{C2-O}(r)$ for $[C_2mIm^+][TFSA^-]$ is the shortest of 3.4 Å, though those in other $g_{Cn-O}(r)$s are located at around 3.5 Å. The stronger nearest neighboring cation−anion interaction in $[C_2mIm^+][TFSA^-]$ relative to that in $[C_3mPyrro^+][TFSA^-]$ is thus attributed to the imidazolium C2H···O ($TFSA^-$) interactions.

In addition, as the representative of the $g_{C9-F}(r)$ for $[C_3mPyrro^+][TFSA^-]$, it can be pointed out that a fluorine of $TFSA^-$ prefers the alkyl chains rather than the ring carbons; i.e., for both ionic liquids, the $g_{Cn-F}(r)$ for the terminal carbon yields the most intense peak among others, and the first peak intensity of $g_{Cn-F}(r)$ indicates a noticeable trend that those for the alkyl chain are similar or rather higher than those for the ring carbons. This may be ascribed to the charge density at the respective atom surface. Supposing that we can estimate such a physically non-observable value with force field parameters, the $|q|/(\sigma/2)^2$ value for the $TFSA^-$ oxygen of 0.242 e $Å^{-2}$ is larger than that for the fluorine of 0.0735 e $Å^{-2}$. In this context, the $TFSA^-$ oxygen may be "*harder*" than the fluorine, though ε of the LJ parameter for the oxygen of 0.879 kJ mol^{-1} is larger than that for the fluorine of 0.276 kJ mol^{-1}. Interestingly, the HSAB concept[148,149] operates at an atomistic level in the closest ion−ion interaction in neat ionic liquids, from which it is supposed that the HSAB concept may have a more important role in the ionic liquids containing softer sulfur or phosphorus atoms.[139,150]

The spatial distribution function (SDF) is useful for comparing the cation−anion interactions between $[C_2mIm^+][TFSA^-]$ and $[C_3mPyrro^+][TFSA^-]$, and the respective one is shown in Figure 5. SDFs for both ionic liquids are similar with those previously reported by other researchers.[102,110,147] The SDF for $[C_2mIm^+][TFSA^-]$ has already been discussed in our previous paper;[69] thus, here we focus on that for $[C_3mPyrro^+][TFSA^-]$. Clearly, the SDF for $[C_3mPyrro^+][TFSA^-]$ is quite different from that for the other, as expected. $TFSA^-$ anions are located near the CH_2 groups directly connected with ammonium nitrogen, possibly due to the relatively larger positive charge at these groups. In addition, it is clear that higher $TFSA^-$ probability around the *N*-methyl group can be attributed to the more extensive spatial availability around it. It is also pointed out that no significant probability of $TFSA^-$ is found around the terminal methyl group in the propyl group. This indicates that a nano-segregated liquid structure of ionic liquids is formed even in $[C_3mPyrro^+][TFSA^-]$ (Figure S4, Supporting Information), as well as $[C_4mPyrro^+][TFSA^-]$.[70]

When considering the ion−ion interaction in the liquid state ionic liquids, the Hildebrand solubility parameter and/or the heat of vaporization were useful, and their values for the imidazolium based ionic liquids are widely available,[151−159] and well reviewed recently.[8,160] However, the heat of vaporization of the pyrrolidinium based ionic liquids has been solely reported for $[C_4mPyrro^+][DCA^-]$ (DCA: dicyanoamide) of 159 kJ mol^{-1} with the aid of high-level ab initio calculations.[161] The same authors also reported the value of 157 kJ mol^{-1} for $[C_4mIm^+][DCA^-]$ with the temperature dependence of the vapor pressure. MD simulations by Borodin well supported this experimental data.[105,106] For instance, the heats of vaporization are 125.9 and 133.2 kJ mol^{-1} for $[C_2mIm^+][DCA^-]$ and $[C_2mPyrro^+][DCA^-]$, respectively, and 133.0 and 147.6 kJ mol^{-1} for $[C_4mIm^+][TFSA^-]$ and $[C_4mPyrro^+][TFSA^-]$. From the viewpoint of heat of vaporization, it seems to be inconsistent with our structural results. However, taking it into consideration that ionic liquids have the nanoscale heterogeneity,[162−166] this discrepancy may be understood.

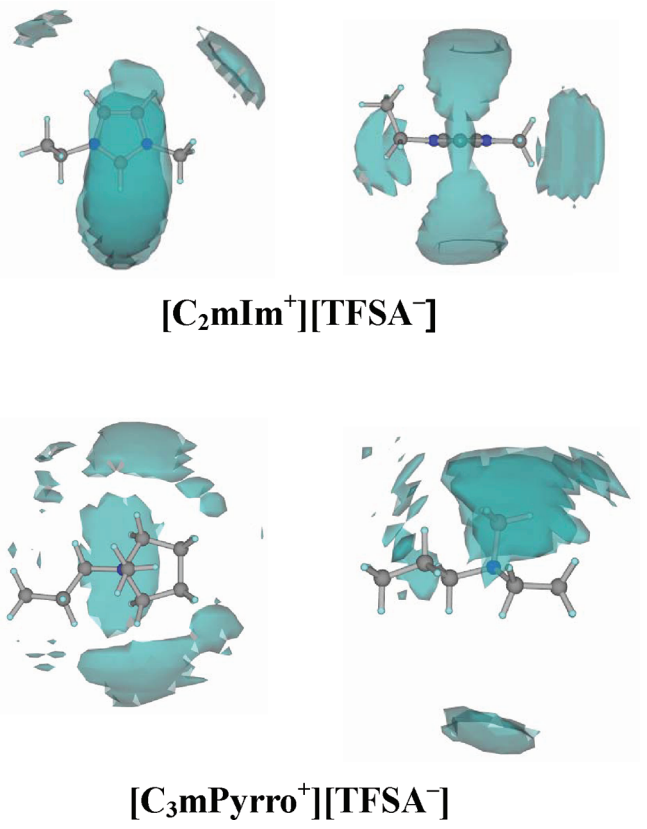

Figure 5. Spatial distribution functions of center-of-mass of $TFSA^-$ around the C2 carbon of $[C_2mIm^+][TFSA^-]$ (upper) and around the ammonium nitrogen of $[C_3mPyrro^+][TFSA^-]$ (lower). Blue clouds around the cation correspond to the 2-fold iso-probability surface relative to the bulk one for the center-of-mass of $TFSA^-$.

According to direct calorimetric determinations of the heat of vaporization of a series of $[C_nmIm^+][TFSA^-]$,[155] the increase of 8.9 kJ mol^{-1} per each CH_2 group can be attributed to an increase in the van der Waals interactions, probably due to the alkyl chain aggregation in nonpolar domains in these ionic liquids. The value is comparable with the difference of 15.9 kJ mol^{-1} between the theoretical heat of vaporization for $[C_2mIm^+][TFSA^-]$ (127.7 kJ mol^{-1}) and $[C_3mPyrro^+][TFSA^-]$ (143.6 kJ mol^{-1}).[105,106] This implies that $[C_3mPyrro^+][TFSA^-]$ has the alkyl chain aggregation but $[C_2mIm^+][TFSA^-]$ does not. In fact, our MD simulations show noticeable intermolecular atom−atom correlation of the C9 in $[C_3mPyrro^+][TFSA^-]$, while the corresponding C8−C8 one is not significant in $[C_2mIm^+][TFSA^-]$, as shown in Figure S4 (Supporting Information). In addition, the first sharp diffraction peaks have been found in the $S(Q)$ for $Q < 0.5$ $Å^{-1}$ for $[C_nmPyrro^+][TFSA^-]$ ionic liquids with $n = 6$, 8, and 10, which suggests that these 1-alkyl-1-methylpyrrolidinium ionic liquids have nanoscale heterogeneity, like the 1-alkyl-3-methylimidazolium ones.[143]

From a dynamic viewpoint, Walden plots of $\log(\Lambda)$ versus $\log(\eta^{-1})$ for ionic liquids, where Λ and η represent the ordinary means, are extensively available and provide a qualitative measure of the ion−ion interaction in ionic liquids[167−170] as well as traditional electrolyte solutions. The difference in the ion−ion interactions between the imidazolium and pyrrolidinium based ionic liquids are unclear, though effort is also made toward a more quantitative approach based on the Walden plot.[171,172] Watanabe et al. proposed

"*ionicity*" as the measure of the ion−ion interactions in ionic liquids (defined as $\Lambda_{imp}/\Lambda_{NMR}$, where Λ_{imp} and Λ_{NMR} stand for the ionic conductivity measured by the ordinary electrochemical AC impedance method and that estimated from the PGSE NMR diffusion coefficients via the Nernst−Einstein equation).[5,173−177] The $\Lambda_{imp}/\Lambda_{NMR}$ values of 0.70[175] and 0.70[178] at 303 K have been reported for $[C_2mIm^+][TFSA^-]$, whereas 0.61 at 298 K[179] and 0.65 at 298 K[36] have been obtained for $[C_3mPyrro^+][TFSA^-]$, which means that the ion−ion interactions in $[C_2mIm^+][TFSA^-]$ may be weaker than those in $[C_3mPyrro^+][TFSA^-]$. Here, again we note the ionic liquid structural heterogeneity; hence, it may be better to compare the cations with the same alkyl chain length. A value of 0.61 for $[C_4mIm^+][TFSA^-]$ shows the ion−ion interaction in this ionic liquid compared with a value of 0.70 for $[C_4mPyrro^+][TFSA^-]$ at 303 K,[176] which qualitatively agrees with our structural results. Furthermore, ab initio calculations for the isolated ion pairs of ionic liquid composing ions by Tsuzuki et al.[180] well support Watanabe's ionicity parameters, and the conclusion deduced in this study.

As is well-known, Watanabe's ionicity parameter $\Lambda_{imp}/\Lambda_{NMR}$ based on the unmodified Nernst−Einstein equation corresponds to $(1-\Delta)$ found in the modified Nernst−Einstein equation, where Δ represents the deviation from the ideal Nernst−Einstein behavior. More generally, it is well established that ion transport properties such as ionic conductivity and ionic diffusion coefficient for electrolyte solutions and molten salts have a relationship to velocity correlation coefficients (VCCs) of the linear response theory.[181] VCCs of several ionic liquids have been reported under atmospheric[36] and elevated pressure.[182−184] It can be said that Watanabe's ionicity parameter is the measure of the ion−ion interactions based on the correlated translational motions among the ions in ionic liquids. In addition, as is also well established, self-diffusion coefficient and ionic conductivity can be evaluated via time dependent mean square displacements and/or velocity correlation functions, and the values corresponding to Watanabe's ionicity have been estimated for a variety of ionic liquids by MD simulations.[102,103,105,108,110] According to Borodin's MD simulations, the values corresponding to Watanabe's ionicity were evaluated to be 0.72 and 0.97 for $[C_2mIm^+][TFSA^-]$ and $[C_3mPyrro^+][TFSA^-]$, respectively, which are in agreement with our structural views but inconsistent with the experimental values aforementioned. Thus, more experimental and theoretical efforts are needed to clarify a molecular picture of Watanabe's ionicity (or $(1-\Delta)$ factor in the modified Nernst−Einstein equation).

Li^+ Ion Solvation Structure in Ionic Liquids. $S^{HEXRD}(Q)$s for the respective ionic liquid with dissolved LiTFSA salt are shown in Figure 6 at the low Q range of $Q < 2.5$ Å^{-1}. Those in the whole Q range examined are also shown in Figure S5 (Supporting Information). In the higher Q range, Li^+ ion dissolution in the ionic liquids hardly affects $S^{HEXRD}(Q)$ owing to the smaller X-ray scattering ability of Li^+ ion. On the other hand, considerable changes caused by the Li^+ ion addition were found in the lower Q-range, as clearly shown in Figure 6. With increasing Li^+ ion mole fraction x_{Li}, $S^{HEXRD}(Q)$s for both ionic liquids were remarkably weakened in intensity at around 0.9 Å^{-1}, where the first peak appeared in the neat ionic liquids. Simultaneously, the first peak in both $S^{HEXRD}(Q)$s shifted toward lower Q-region when Li^+ ion was added. In addition, small but significant variations can be found; i.e., both $S^{HEXRD}(Q)$s were intensified in intensity at around 0.7 and 1.25 Å^{-1} and weakened below 0.5 Å^{-1}. As well as the first peak, the second peak observed in both neat ionic liquids shifted toward lower Q-range as the increase of x_{Li}. All of these observations evidently suggest that the larger structure is formed in the ionic liquids when dissolving Li^+ ion.

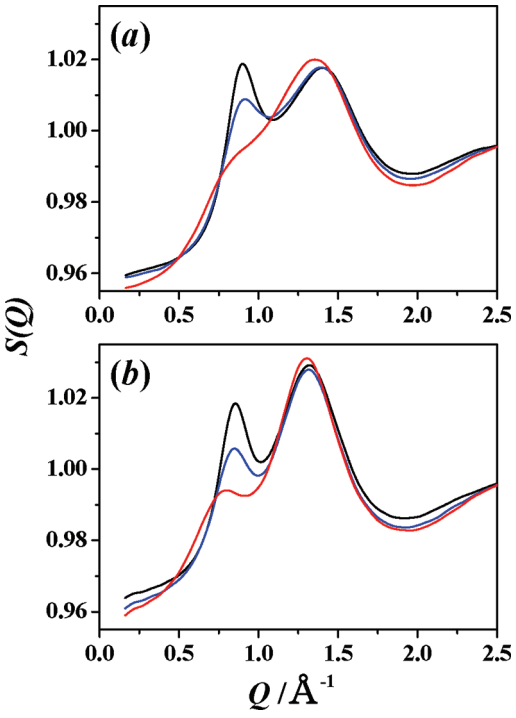

Figure 6. Observed X-ray structure functions at 298 K for $[Li^+]_x[C_2mIm^+]_{(1-x)}[TFSA^-]$ (upper) and $[Li^+]_x[C_3mPyrro^+]_{(1-x)}[TFSA^-]$ (lower) at the Q range of $0 < Q/Å^{-1} < 2.5$, respectively. Black, blue, and red lines represent $x = 0.0$, 0.15, and 0.32, respectively.

$G^{HEXRD}(r)$s for both ionic liquids are shown in Figure 7. Peaks observed in $G^{HEXRD}(r)$ of the r range can be mainly ascribable to the intramolecular atom−atom correlations as previously discussed elsewhere.[69,70] For both ionic liquids, as expected from $S^{HEXRD}(Q)$ of higher Q-range, variation in $G^{HEXRD}(r)$ caused by the Li^+ ion dissolution was minor. As shown in the inserted figures, however, noticeable and systematic changes as the increase of x_{Li} can be found for the second peak in $G^{HEXRD}(r)$ of $[C_2mIm^+][TFSA^-]$ even the experimental errors were taken into consideration, while little significant variation observed in $G^{HEXRD}(r)$ for $[C_3mPyrro^+][TFSA^-]$. For $[C_2mIm^+][TFSA^-]$, with increasing x_{Li}, the second peak of about 1.78 Å observed for the neat ionic liquid decreased in intensity, while the alternative larger second peak of about 1.9 Å appeared, and was intensified. Nevertheless, such variations were unclear for $[C_3mPyrro^+][TFSA^-]$, probably due to the second peak of about 1.85 Å located even in the neat ionic liquid.

As already mentioned, Li^+ ion solvation in various ionic liquids has been well studied by Raman spectroscopy,[20−24,65,66,68] and it has become well established that the Li^+ ion in the TFSA based ionic liquids is solvated by two $TFSA^-$ anions and has a 4-fold coordinated structure in $x_{Li} < 0.2$. In addition, according to a recent Raman spectroscopic study by Lassègues et al., it has been elucidated that an apparent Li^+ ion solvation number in the TFSA based ionic liquid decreases from 2 at a higher x_{Li}, indicating the formation of oligomers consisting of multiple Li^+ ions and $TFSA^-$ anions.[24] Moreover, structural parameters such as the Li^+−O bond length and the coordination number have been accumulated for the solvated Li^+ ion in aqueous and nonaqueous

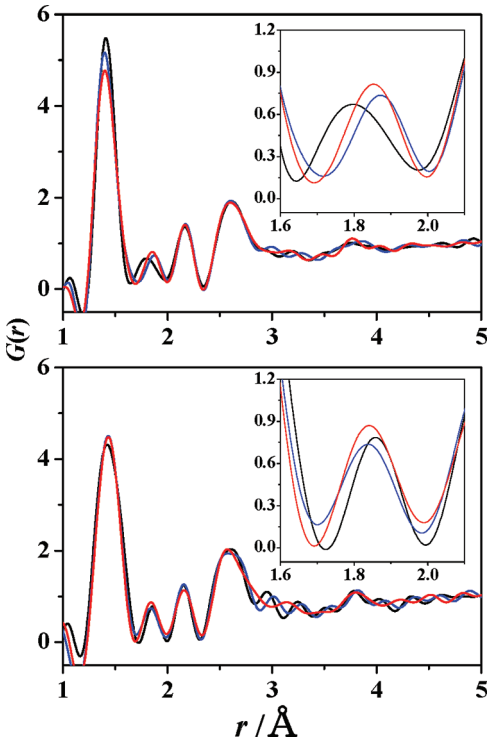

Figure 7. Observed X-ray radial distribution functions $G(r)$ for $[Li^+]_x[C_2mIm^+]_{(1-x)}[TFSA^-]$ (upper) and $[Li^+]_x[C_3mPyrro^+]_{(1-x)}[TFSA^-]$ (lower) at the r range of $0 < r/Å < 6$ at 298 K, respectively. Line colors correspond to those in Figure 6. Inserted figures are the respective zoomed up one at the r range of $1.6 < r/Å < 2.1$.

solvent solutions except ionic liquids.[42−51] From this literature, it is considered that the 4-fold coordinated Li^+ ion predominantly exists as its solvation structure with the bond length ranging from 1.9 to 2.1 Å in most solvents solvating with a monodentate manner.

Taking such accumulated knowledge on the Li^+ ion solvation structures in molecular and ionic liquids into consideration, it can be deduced that the Li^+−O ($TFSA^-$) atom−atom correlations in the Li^+ ion solvated cluster $[Li(TFSA)_2]^+$ contribute to the newly appeared peak of about 1.9 Å in $G^{HEXRD}(r)$ for $[C_2mIm^+][TFSA^-]$, although the distance is slightly shorter compared with the above-mentioned Li^+−O bond length ranging from 1.9 to 2.1 Å in aqueous and nonaqueous solvent solutions. The bond length of the Li^+−O (solvent) in solution depends on the solvent properties such as electron pair donating ability, Lewis and/or Brønsted basicity, and also solvating manner such as mono- or multidentate ones. Some sorts of solvent parameters as a measure of such natures of ionic liquids are now available; the Lewis basicity probed by UV−vis absorption spectra of the Cu(II) complex,[177,185,186] the autodissociation constant in neat ionic liquids based on directly measured pH by potentiometry,[187−190] and the gas phase acidity of the conjugated Brønsted acid of the anions.[191,192] However, it should be noted that $TFSA^-$ acts as a bidentate molecular solvent like glyme and others.[193−196] It is difficult to discuss the structure−property relationships between the Li^+ ion solvation in the $TFSA^-$ based ionic liquids quantitatively at the present stage. One of the reasons why arises from the lack of knowledge on the bidentate solvent even in molecular nonaqueous solvents.[197−199] For the bidentate ligand, conformational changes caused by chelation or chelated ring distortion may seriously contribute in stabilization energy, so that the Li^+−O distance in the chelated ring should depend on such energetic disadvantage. More experimental efforts will be necessary to reveal the Li^+ ion solvation structure not only in ionic liquids but also in ordinary molecular solvents.

MD simulations for $[C_2mIm^+][TFSA^-]$ containing Li^+ ion were carried out. MD derived $S^{MD}(Q)$s and $G^{MD}(i)$s are shown in Figure S6 (Supporting Information). As can be seen from these figures, MD simulations qualitatively agree with experiments. Though Raman spectroscopic studies have already revealed the number of $TFSA^-$ solvated to the Li^+ ion in ionic liquids of 2,[20−24,65,66,68] larger values were evaluated by MD simulations depending on x_{Li}. Figure S7 (Supporting Information) displays pair correlation functions for the Li^+ ion $g_{Li-X}(r)$s. For instance, with regard to $x_{Li} = 0.15$, coordination numbers estimated from the $g_{Li-O}(r)$ and $g_{Li-S}(r)$ were practically the same values of 5.23 and 5.26. In addition, the closed two peaks of the $Li^+\cdots N$ correlations can be found at 3.60 and 4.33 Å in the $g_{Li-N}(r)$ with coordination numbers of 2.25 and 1.43, respectively, which indicates that at least two kinds of solvated $TFSA^-$ and also Li^+ ion solvated clusters simultaneously exist in simulations; i.e., the closer bidentate and the further monodentate $TFSA^-$, and the Li^+ ions of 4- and 5-fold coordinated structures. Such larger coordination number may yield a slightly longer Li^+−O ($TFSA^-$) distance of about 1.96 Å in MD simulations relative to the experiments. Thus, the Li^+ ion solvated clusters found in our simulations agree well with those found in MD simulations performed by Monteiro et al.[41] In addition, we carried out MD simulations for the same systems at an elevated temperature of 398 K. As previously discussed in our Raman spectroscopic study,[68] the Li^+ ion solvation number is independent from temperature at $x_{Li} < 0.2$. This is consistent with MD simulations, as clearly shown in Figure S7 (Supporting Information), though the apparent solvation number of $TFSA^-$ is different from that established by the experiment. It is worth mentioning the conformational isomerism of the $TFSA^-$ in the Li^+ solvated cluster. Our simulations reproduced the experimental fact[68] that the cis $TFSA^-$ is more stabilized in the Li^+ first solvation sphere relative to the bulk.[67]

As mentioned above, dissolution of Li salt into ionic liquids causes considerable structural variation in long-range ordering of ionic liquids, which is clearly indicated by X-ray radial distribution functions (RDFs) as the form of $r^2\{G(r) - 1\}$ shown in Figure 8. For both ionic liquid solutions containing Li^+ ion, broad peaks of about 6, 10, and 15 Å were observed in the RDFs, which agree well with our previous publications.[69,70] As suggested by X-ray structure factor data, the long-range density fluctuation (oscillation amplitude) of $r > 7.5$ Å decreased with the increase of x_{Li}. In addition, it can be pointed out that the second broad peak at around 9−10 Å attributable to the same sign ion−ion correlations shifted toward longer with increasing lithium ion content. Taking into account the X-ray scattering ability of the respective ion, these variations indicate the anion−anion correlations strongly change from those in the neat ionic liquids. This is consistent with the formation of the lithium ion solvated cluster $[Li(TFSA)_2]^-$. However, it is difficult to discuss quantitatively such long-range ordering in RDFs by sole experimental data. Here, we interpret our experimental finding with the aid of MD simulations. X-ray RDFs from MD simulations can be divided into three components, i.e., RDFs for the $[C_2mIm]-[C_2mIm]$, the $[C_2mIm]-[TFSA]$, and the $[TFSA]-[TFSA]$, respectively. These RDFs are shown in Figure 9. As can be clearly seen in these figures, the observed variation in the long-range ordering of the

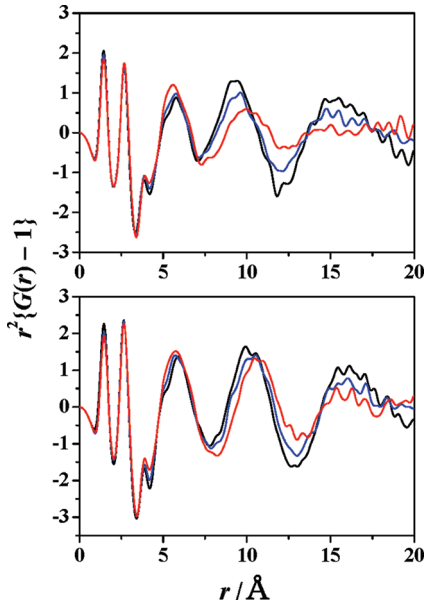

Figure 8. Observed long-range X-ray radial distribution functions as the form of $r^2\{G(r) - 1\}$, in which $G(r)$ was obtained by the Fourier transformation with B = 0.023 in eq 2, for $[Li^+]_x[C_2mIm^+]_{(1-x)}$-$[TFSA^-]$ (upper) and $[Li^+]_x[C_3mPyrro^+]_{(1-x)}[TFSA^-]$ (lower) at the r range of $0 < r/Å < 20$, respectively. Line colors correspond to those in Figure 6.

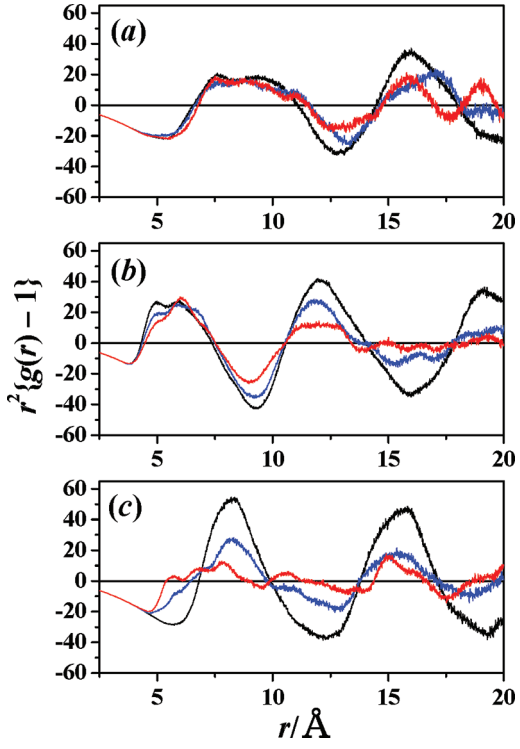

Figure 9. X-ray radial distribution functions as the form of $r^2\{G(r) - 1\}$ for the center-of-mass of cation−cation (a), cation−anion (b), and anion−anion (c), respectively, derived from MD simulations for $[Li^+]_x$-$[C_2mIm^+]_{(1-x)}[TFSA^-]$ (x = 0.0, 0.15, and 0.32). Line colors correspond to those in Figure 6.

ionic liquids can be mainly ascribable to the anion−anion correlation. Highest peaks of about 8.2 and 15.5 Å and deepest valleys of about 12 and 19 Å can be found in the anion−anion RDFs for the neat $[C_2mIm][TFSA]$; they remarkably diminished with the increase of the lithium ion.

It is also pointed out that the peak intensity at around 5 Å in RDFs for the cation−anion decreased with the increase of the lithium ion concentration, while the valley at around 6 Å in the RDF for the anion−anion in the neat ionic liquid turned to the peak at about 5.5 Å. These changes correspond to the formation of the $[Li(TFSA)_2]^-$ accompanied by the collapse of the closest $[C_2mIm]$−$[TFSA]$ correlation in the ionic liquid. However, it should be noted that the closest $[C_2mIm]$−$[TFSA]$ correlation significantly remains as a peak with no practical shift in position at the highest x_{Li} of 0.32. This may indicate the C_2mIm^+ cation interacts with the $[Li(TFSA)_2]^-$ anionic clusters. In fact, pair correlation functions for the Li^+−C2(C_2mIm^+) (Figure S8, Supporting Information) exhibit the first peaks of 7 Å with shoulders of both shorter and longer sides. The first peak of 7 Å can be obviously ascribed to the $[Li(TFSA)_2]^-$−C_2mIm^+ interaction. Such interaction between the $[Li(TFSA)_2]^-$ and C_2mIm^+ is consistent with our previous Raman spectroscopic and ab initio study on the conformational isomerism of $TFSA^-$ in the first solvation sphere of the lithium ion.[68] More detailed structural information of the Li^+ ion solvation in the TFSA based ionic liquids may be obtained by means of neutron diffraction experiments with the $^6Li/^7Li$ isotope substitution technique,[48] and such effort is now going on.

CONCLUSION

To shed more light onto the Li^+ ion solvation structure in the TFSA based ionic liquids, $[C_2mIm][TFSA]$ and $[C_3mPyrro]$-$[TFSA]$ ionic liquids with dissolved LiTFSA salt at a lithium ion mole fraction of x_{Li} = 0.0, 0.15, and 0.3 were explored by means of HEXRD experiments with the aid of MD simulations.

For the neat ionic liquids, rather small but significant differences were found in the intermolecular radial distribution functions for these ionic liquids; i.e., $G_{inter}(r)$ for $[C_2mIm][TFSA]$ locates a shorter position at about 3.5 Å relative to that for $[C_3m$-$Pyrro][TFSA]$, suggesting that the closest cation−anion interaction in the $[C_2mIm][TFSA]$ is stronger than that in the $[C_3mPyrro][TFSA]$. This experimental evidence is consistent with other macroscopic properties or solvent parameters such as the heat of vaporization or solubility parameters and Watanabe's ionicity parameter, if we take into consideration the ionic liquid structural heterogeneity.

For ionic liquids with dissolving Li^+ ion, the peak at about 1.9 Å ascribable to the Li^+−O ($TFSA^-$) correlation appeared in $G(r)$ for $[C_2mIm][TFSA]$, while the corresponding peak could not be found in that for $[C_3mPyrro][TFSA]$ due to the difference in the intramolecular atom−atom correlations among these cations. Moreover, we found that dissolved Li^+ ion into these ionic liquids causes considerable variation in the long-range ordering (density fluctuation or oscillation amplitude) of both ionic liquids. The observed long-range structural variations can be attributed from MD simulations to those in the anion−anion correlation caused by the formation of a large Li^+ ion solvated cluster of $[Li(TFSA)_2]^-$.

ASSOCIATED CONTENT

Supporting Information. Figures S1−S8 showing additional data. This material is available free of charge via the Internet at http://pubs.acs.org.

AUTHOR INFORMATION

Corresponding Author
*E-mail: yumeb@chem.kyushu-univ.jp. Fax: +81 92 642 2582. Phone: +81 92 642 2582.

ACKNOWLEDGMENT

This work has been financially supported by Grant-in-Aids for Scientific Research No. 19003963, 19350033, 20350037, and P10750, and for Scientific Research in Priority Area (Ionic Liquids) 20031024 from the MEXT of Japan and Advanced Low Carbon Technology Research and Development Program (ALCA) from Japan Science and Technology Agency (JST). HEXRD experiments were performed as the subject No. 2006B1286 of SPring-8.

REFERENCES

(1) *Ionic Liquids in Syntheses*, 2nd ed.; Wasserscheid, P., Welton, T., Eds.; VCH-Wiley: Weinheim, Germany, 2007; Vols. 1 and 2.
(2) *Electrochemical Aspects of Ionic Liquids*; Ohno, H., Ed.; Wiley-Interscience: Hoboken, NJ, 2005.
(3) Aparicio, S.; Atilhan, M.; Karadas, F. *Ind. Eng. Chem. Res.* **2010**, *49*, 9580–9595.
(4) Castner, E. W., Jr.; Wishart, J. F. *J. Chem. Phys.* **2010**, *132*, 120901/1–120901/9.
(5) Ueno, K.; Tokuda, H.; Watanabe, M. *Phys. Chem. Chem. Phys.* **2010**, *12*, 1649–1658.
(6) Buchner, R.; Hefter, G. *Phys. Chem. Chem. Phys.* **2009**, *11*, 8984–8999.
(7) Weingärtner, H. *Angew. Chem., Int. Ed.* **2008**, *47*, 654–970.
(8) Ludwig, R.; Krag, U. *Angew. Chem., Int. Ed.* **2007**, *46*, 6582–6584.
(9) Lewandowski, A.; Świderska-Mocek, A. *J. Power Sources* **2009**, *194*, 601–609.
(10) MacFarlane, D. R.; Huang, J.; Forsyth, M. *Nature* **1999**, *402*, 792–794.
(11) Sakaebe, H.; Matsumoto, H. *Electrochem. Commun.* **2003**, *5*, 594.
(12) Katayama, Y.; Yukumoto, M.; Miura, T. *Electrochem. Solid-State Lett.* **2003**, *6*, A96.
(13) Garcia, B.; Lavallee, S.; Perron, G.; Michot, C.; Armand, M. *Electrochim. Acta* **2004**, *49*, 4583.
(14) Abe, T.; Fukuda, H.; Iriyama, Y.; Ogumi, Z. *J. Electrochem. Soc.* **2004**, *151*, A1120–A1123.
(15) Park, M.; Zhang, X.; Chung, M.; Less, G. B.; Sastry, A. M. *J. Power Sources* **2010**, *19*, 7904–7929.
(16) Johansson, P.; Gejji, S. P.; Tegensfeldt, J.; Lindgren, J. *Electrochim. Acta* **1998**, *43*, 1375.
(17) Herstedt, M.; Smirnov, M.; Johansson, P.; Chami, M.; Grondin, J.; Servant, L.; Lassègues, J.-C. *J. Raman Spectrosc.* **2005**, *36*, 762.
(18) Herstedt, M.; Henderson, W. A.; Smirnov, M.; Ducasse, L.; Servant, L.; Talaga, D.; Lassègues, J.-C. *J. Mol. Struct.* **2006**, *783*, 145.
(19) Lassègues, J.-C.; Grondin, J.; Holomb, R.; Johansson, P. *J. Raman Spectrosc.* **2007**, *38*, 551–558.
(20) Castriota, M.; Caruso, T.; Agostino, R. G.; Cazzanelli, E.; Henderson, W. A.; Passerini, S. *J. Phys. Chem. A* **2005**, *109*, 92–96.
(21) Lassègues, J.-C.; Grondin, J.; Talaga, D. *Phys. Chem. Chem. Phys.* **2006**, *8*, 5629.
(22) Hardwick, L. J.; Holzapfel, M.; Wokaun, A.; Novák, P. *J. Raman Spectrosc.* **2007**, *38*, 110.
(23) Duluard, S.; Grondin, J.; Bruneel, J.-L.; Pianet, I.; Grélard, A.; Campet, G.; Delville, M.-H.; Lassègues, J.-C. *J. Raman Spectrosc.* **2008**, *39*, 627.
(24) Lassègues, J.-C.; Grondin, J.; Aupetit, C.; Johansson, P. *J. Phys. Chem. A* **2009**, *113*, 305.
(25) Hayamizu, K.; Aihara, Y.; Nakagawa, H.; Nukuda, T.; Price, W. S. *J. Phys. Chem. B* **2004**, *108*, 19527.
(26) Nicotera, I.; Oliviero, C.; Henderson, W. A.; Appetecchi, G. B.; Passerini, S. *J. Phys. Chem. B* **2005**, *109*, 22814.
(27) Ye, H.; Huang, J.; Xu, J. J.; Khalfan, A.; Greenbaum, S. G. *J. Electrochem. Soc.* **2007**, *154*, A1048.
(28) Saito, Y.; Umecky, T.; Niwa, J.; Sakai, T.; Maeda, S. *J. Phys. Chem. B* **2007**, *111*, 11794.
(29) Umecky, T.; Saito, Y.; Okumura, Y.; Maeda, S.; Sakai, T. *J. Phys. Chem. B* **2008**, *112*, 3357.
(30) Hayamizu, K; Tsuzuki, S; Seki, S.; Ohno, Y.; Miyashiro, H.; Kobayashi, Y. *J. Phys. Chem. B* **2008**, *112*, 1189.
(31) Frömling, T; Kunze, M.; Schönhoff, M.; Sundermeyer, J.; Roling, B. *J. Phys. Chem. B* **2008**, *112*, 12985.
(32) Hayamizu, K.; Tsuzuki, S.; Seki, S. *J. Phys. Chem. A* **2008**, *112*, 12027.
(33) Umecky, T; Saito, Y; Matsumoto, H. *J. Phys. Chem. B* **2009**, *113*, 8466.
(34) Phung Le, M.-L.; Alloin, F.; Strobel, P.; Leprêtre, J.-C; del Valle, C. P.; Judeinstein, P. *J. Phys. Chem. B* **2010**, *114*, 894–903.
(35) Kunze, M.; Montanino, M.; Appetecchi, G. B.; Jeong, S.; Schönhoff, M.; Winter, M.; Passerini, S. *J. Phys. Chem. A* **2010**, *114*, 1776.
(36) Hayamizu, K.; Tsuzuki, S.; Seki, S.; Fujii, K.; Suenaga, M.; Umebayashi, Y. *J. Chem. Phys.* **2010**, *133*, 194505.
(37) Nicolau, B. G.; Sturlaugson, A.; Fruchey, K.; Ribeiro, M. C. C.; Fayer, M. D. *J. Phys. Chem. B* **2010**, *114*, 8350–8356.
(38) Gejji, S. P.; Suresh, C. H.; Babu, K.; Gadre, S. R. *J. Phys. Chem. A* **1999**, *103*, 7474.
(39) Tsuzuki, S.; Hayamizu, K.; Seki, S.; Ohno, Y.; Kobayashi, Y.; Miyashiro, H. *J. Phys. Chem. B* **2008**, *112*, 9914.
(40) Borodin, O.; Smith, G. D.; Henderson, W. *J. Phys. Chem. B* **2006**, *110*, 16879.
(41) Monteiro, M. J.; Bazito, F. F. C.; Siqueira, L. J. A.; Ribeiro, M. C. C.; Torresi, R. M. *J. Phys. Chem. B* **2008**, *112*, 2102.
(42) Smirnov, P. R.; Trostin, V. N. *Russ. J. Gen. Chem.* **2006**, *76*, 175.
(43) Kameda, Y.; Sasaki, M.; Amo, Y.; Usuki, T. *Bull. Chem. Soc. Jpn.* **2006**, *79*, 228.
(44) Kameda, Y.; Mochiduki, K.; Imano, M.; Naganuma, H.; Sasaki, M.; Amo, Y.; Usuki, T. *J. Mol. Liq.* **2005**, *119*, 159.
(45) Kameda, Y.; Imano, M.; Takeuchi, M.; Suzuki, S.; Usuki, T.; Uemura, O. *J. Non-Cryst. Solids* **2001**, *293−295*, 600.
(46) Kameda, Y.; Ebata, H.; Uemura, O. *Bull. Chem. Soc. Jpn.* **1994**, *67*, 929.
(47) Kameda, Y.; Uemura, O. *Bull. Chem. Soc. Jpn.* **1993**, *66*, 384.
(48) Kameda, Y.; Umebayashi, Y.; Takeuchi, M.; Wahab, M. A.; Fukuda; Ishiguro, S.; Sasaki, M.; Amo, Y.; Usuki, T. *J. Phys. Chem. B* **2007**, *111*, 6104.
(49) Kameda, Y.; Kudoh, N.; Suzuki, S.; Usuki, T.; Uemura, O. *Bull. Chem. Soc. Jpn.* **2001**, *74*, 1009.
(50) Kameda, Y.; Ebata, H.; Usuki, T.; Uemura, O. *Physica B* **1995**, *213/214*, 477.
(51) Cartailler, T.; Kunz, W.; Turq, P.; Bellisent-Funel, M.-C. *J. Phys.: Condens. Matter* **1991**, *3*, 9511.
(52) Chong, S.-H.; Hirata, F. *J. Chem. Phys.* **1999**, *111*, 3654–3667.
(53) Koneshan, S.; Rasaiah, J. C.; Lynden-Bell, R. M.; Lee, S. H. *J. Phys. Chem.* **1998**, *102*, 4193–4204.
(54) Yamaguchi, T.; Hirata, F. *J. Chem. Phys.* **2001**, *115*, 9340–9345.
(55) Chong, S.-H.; Goetze, W. *Phys. Rev.* **2002**, *E65*, 041503.
(56) Yamaguchi, T.; Matsuoka, T.; Koda, S. *J. Chem. Phys.* **2007**, *127*, 234501.
(57) Matsumoto, K.; Tsuda, T.; Hagiwara, R.; Ito, Y.; Tamada, O. *Solid State Sci.* **2002**, *4*, 23–26.
(58) Matsumoto, K.; Hagiwara, R.; Yoshida, R.; Ito, Y.; Mazej, Z.; Benkič, P.; Žemva, B.; Tamada, O.; Yoshino, H.; Matsubara, S. *Dalton Trans* **2004**, 144–149.
(59) Dean, P. M.; Pringle, J. M.; MacFarlane, D. R. *Phys. Chem. Chem. Phys.* **2010**, *12*, 9144–9153.
(60) Fujii, K.; Kanzaki, R.; Takamuku, T.; Fujimori, T.; Umebayashi, Y.; Ishiguro, S. *J. Phys. Chem. B* **2006**, *110*, 8179.
(61) Fujii, K.; Seki, S.; Fukuda, S.; Kanzaki, R.; Takamuku, T.; Umebayashi, Y; Ishiguro, S. *J. Phys. Chem. B* **2007**, *111*, 12829–12833.

(62) Lopes, J. N. C.; Shimizu, K.; Pádua, A. A. H.; Umebayashi, Y.; Fukuda, S.; Fujii, K.; Ishiguro, S. *J. Phys. Chem. B* **2008**, *112*, 1465–1472.
(63) Lopes, J. N. C.; Shimizu, K.; Padua, A. A. H.; Umebayashi, Y.; Fujii, K.; Fukuda, S.; Ishiguro, S. *J. Phys. Chem. B* **2008**, *112*, 9449–9455.
(64) Fujii, K.; Shiro, S.; Fukuda, S.; Takamuku, T.; Kohara, S.; Kameda, Y.; Umebayashi, Y.; Ishiguro, S. *J. Mol. Liq.* **2008**, *143*, 64–69.
(65) Umebayashi, Y.; Mitsugi, T.; Fukuda, S.; Fujimori, T.; Fujii, K.; Kanzaki, R.; Takeuchi, M.; Ishiguro, S. *J. Phys. Chem. B* **2007**, *111*, 13028–13032.
(66) Shirai, A.; Fujii, K.; Seki, S.; Umebayashi, Y.; Ishiguro, S.; Ikeda, Y. *Anal. Sci.* **2008**, *24*, 1291.
(67) Umebayashi, Y.; Yamaguchi, T.; Fukuda, S.; Mitsugi, T.; Takeuchi, M.; Fujii, K.; Ishiguro, S. *Anal. Sci.* **2008**, *24*, 1297–1304.
(68) Umebayashi, Y.; Mori, S.; Fujii, K.; Tsuzuki, S.; Seki, S.; Hayamizu, K.; Ishiguro, S. *J. Phys. Chem. B* **2010**, *114*, 6513–6521.
(69) Fujii, K.; Soejima, Y.; Kyoshoin, Y.; Fukuda, S.; Kanzaki, R.; Umebayashi, Y.; Yamaguchi, T.; Ishiguro, S.; Takamuku, T. *J. Phys. Chem. B* **2008**, *112*, 4329–4336.
(70) Fukuda, S.; Takeuchi, M.; Fujii, K.; Kanzaki, R.; Takamuku, T.; Chiba, K.; Yamamoto, H.; Umebayashi, Y.; Ishiguro, S. *J. Mol. Liq.* **2008**, *143*, 2–7.
(71) Umebayashi, Y.; Chung, W.-L.; Mitsugi, T.; Fukuda, S.; Takeuchi, M.; Fujii, K.; Takamuku, T.; Kanzaki, R.; Ishiguro, S. *J. Comput. Chem., Jpn.* **2008**, *7*, 125–134.
(72) Fujii, K.; Mitsugi, T.; Takamuku, T.; Yamaguchi, T.; Umebayashi, Y.; Ishiguro, S. *Chem. Lett.* **2009**, *38*, 340–341.
(73) Kanzaki, R.; Mitsugi, T.; Fukuda, S.; Fujii, K.; Takeuchi, M.; Soejima, Y.; Takamuku, T.; Yamaguchi, T.; Umebayashi, Y.; Ishiguro, S. *J. Mol. Liq.* **2009**, *147*, 77–82.
(74) Umebayashi, Y.; Hamano, H.; Tsuzuki, S.; Lopes, J. N. C.; Pádua, A. A. H.; Kameda, Y.; Kohara, S.; Yamaguchi, T.; Fujii, K.; Ishiguro, S. *J. Phys. Chem. B* **2010**, *114*, 11715–11724.
(75) Nockemann, P.; Binnemans, K.; Driesen, K. *Chem. Phys. Lett.* **2005**, *415*, 131.
(76) Earle, M. J.; Gordon, C. M.; Plechkova, N. V.; Seddon, K. R.; Welton, T. *Anal. Chem.* **2007**, *79*, 758.
(77) Burrel, A. R.; Del Sasto, R. E.; Baker, S. N.; McCleskey, T. M.; Baker, G. A. *Green Chem.* **2007**, *9*, 449.
(78) Isshiki, M.; Ohishi, Y.; Goto, S.; Takeshita, K.; Takeshita, K.; Ishikawa, T. *Nucl. Instrum. Methods Phys. Res., Sect. A* **2001**, *467−468*, 663.
(79) Kohara, S.; Suzuya, K.; Kashihara, Y.; Matsumoto, N.; Umesaki, N.; Sakai, I. *Nucl. Instrum. Methods Phys. Res., Sect. A* **2001**, *467−468*, 1030.
(80) Sasaki, S. KEK Report 90-16, National Laboratory for High Energy Physics, Japan, 1991.
(81) Hubbell, J. H.; Veigele, W. J.; Briggs, E. A.; Brown, R. T.; Cromer, D. T.; Howerton, R. J. *J. Phys. Chem. Ref. Data* **1975**, *4*, 471.
(82) Cromer, D. T. *J. Chem. Phys.* **1969**, *50*, 4857.
(83) Cormer, D. T.; Mann, J. B. *J. Chem. Phys.* **1967**, *47*, 1892.
(84) Maslen, E. N.; Fox, A. G.; O'Keefe, M. A. *International Tables For Crystallography Vol. C*; Kluwer: Dordrecht, The Netherlands, 1999; pp 572−574.
(85) Johanson, G.; Sandstörm, M. *Chem. Scr.* **1973**, *4*, 195.
(86) Jorgensen, W. L.; Maxwell, D. S.; Tirado-Rives, J. *J. Am. Chem. Soc.* **1996**, *118*, 11225.
(87) Kaminski, G.; Jorgensen, W. L. *J. Phys. Chem.* **1996**, *100*, 18010.
(88) Lopes, J. N. C.; Deschamps, J.; Pádua, A. A. H. *J. Phys. Chem. B* **2004**, *108*, 2038–2047.
(89) Lopes, J. N. C.; Pádua, A. A. H. *J. Phys. Chem. B* **2004**, *108*, 16893–16898.
(90) Lopes, J. N. C.; Pádua, A. A. H. *J. Phys. Chem. B* **2006**, *110*, 19586–19592.
(91) Lopes, J. N. C.; Pádua, A. A. H.; Shimizu, K. *J. Phys. Chem. B* **2008**, *112*, 5039–5046.
(92) Shimizu, K; Almantariotis, D.; Gomes, M. F. C.; Pádua, A. A. H.; Lopes, J. N. C. *J. Phys. Chem. B* **2010**, *114*, 3592–3600.
(93) Bhargava, B. L.; Balasubramanian, S.; Klein, M. L. *Chem. Commun.* **2008**, 3339–3351.
(94) Maginn, E. J. *J. Phys.: Condens. Matter* **2009**, *21*, 373101.
(95) Sambasivarao, S. V.; Acevedo, O. *J. Chem. Theory Comput.* **2009**, *5*, 1038–1050.
(96) Tsuzuki, S.; Shinoda, W.; Saito, H.; Mikami, M.; Tokuda, H.; Watanabe, M. *J. Phys. Chem. B* **2009**, *113*, 10641–10649.
(97) Köddermann, T.; Paschek, D.; Ludwig, R. *ChemPhysChem* **2008**, *9*, 549–555.
(98) Köddermann, T.; Paschek, D.; Ludwig, R. *ChemPhysChem* **2007**, *8*, 2464–2470.
(99) Zhao, W.; Eslami, H.; Cavalcanti, W. L.; Müller-Plathe, F. *Z. Phys. Chem.* **2007**, *221*, 1647–1662.
(100) Bhargavaa, B. L.; Balasubramanian, S. *J. Chem. Phys.* **2007**, *127*, 114510/1–114510/6.
(101) Wu, X.; Liu, Z.; Huang, S.; Wang, W. *Phys. Chem. Chem. Phys.* **2005**, *7*, 2771–2779.
(102) Borodin, O.; Smith, G. D. *J. Phys. Chem. B* **2006**, *110*, 11481–11490.
(103) Borodin, O.; Smith, G. D.; Henderson, W. *J. Phys. Chem. B* **2006**, *110*, 16879–16886.
(104) Smith, G. D.; Borodin, O.; Li, L.; Kim, H.; Liu, Q.; Bara, J. E.; Gin, D. L.; Nobel, R. *Phys. Chem. Chem. Phys.* **2008**, *10*, 6301–6312.
(105) Borodin, O. *J. Phys. Chem. B* **2009**, *113*, 11463–11478.
(106) Borodin, O. *J. Phys. Chem. B* **2009**, *113*, 12353–12357.
(107) Borodin, O.; Smith, G. D.; Kim, H. *J. Phys. Chem. B* **2009**, *113*, 4771–4774.
(108) Hooper, J. B.; Borodin, O. *Phys. Chem. Chem. Phys.* **2010**, *12*, 4635–4643.
(109) Bedrov, D.; Borodin, O.; Li, Z.; Smith, G. D. *J. Phys. Chem. B* **2010**, *114*, 4984–4997.
(110) Borodin, O; Gorecki, W.; Smith, G. D.; Armand, M. *J. Phys. Chem. B* **2010**, *114*, 6786–6798.
(111) Bedrov, D.; Borodin, O. *J. Phys. Chem. B* **2010**, *114*, 12802–12810.
(112) Soetens, J.-C.; Millot, C.; Maigret, B. *J. Phys. Chem. A* **1998**, *102*, 1055–1061.
(113) Joung, I.-S.; Cheatham, T. E., III. *J. Phys. Chem. B* **2008**, *112*, 9020–9041.
(114) Gear, G. W. *Numerical Initial Value Problems in Ordinary Differential Equations*; Prentice-Hall, Inc.: 1971.
(115) Berendsen, H. J. C.; Van Gunsteren, W. F. In *Proceeding of the Enrico Fermi Summer School on Molecular dynamics simulation of statistical mechanical system*; Ciccotti, G., Hover, G., Eds.; North Holland: 1986; p 43.
(116) Nose, S. *Mol. Phys.* **1984**, *52*, 255.
(117) Nose, S. *J. Chem. Phys.* **1984**, *81*, 511.
(118) Parrinello, M.; Rahman, A. *J. Appl. Phys.* **1981**, *52*, 7182.
(119) Parrinello, M.; Rahman, A. *Phys. Rev. Lett.* **1980**, *45*, 1196.
(120) Umebayashi, Y.; Fujimori, T.; Sukizaki, T.; Asada, M.; Fujii, K.; Kanzaki, R.; Ishiguro, S. *J. Phys. Chem. A* **2005**, *109*, 8976–8982.
(121) Umebayashi, Y.; Mitsugi, T.; Fujii, K.; Seki, S.; Chiba, K.; Yamamoto, H.; Lopes, J. N. C.; Pádua, A. A. H.; Takeuchi, M.; Kanzaki, R.; Ishiguro, S. *J. Phys. Chem. B* **2009**, *113*, 4338–4346.
(122) Lopes, J. N. C.; Pádua, A. A. H. *J. Phys. Chem. B* **2006**, *110*, 7485–7489.
(123) Takahashi, S.; Suzuya, K.; Kohara, S.; Koura, N.; Curuism, L. A.; Saboungi, M.-L. *Z. Phys. Chem.* **1999**, *209*, 209–221.
(124) Morita, H.; Kohara, S.; Usuki, T. *J. Mol. Liq.* **2009**, *147*, 182–185.
(125) Hagiwara, R.; Matsumoto, K.; Tsuda, T.; Ito, Y.; Kohara, S.; Suzuya, K.; Matsumoto, H.; Miyazaki, Y. *J. Non-Cryst. Solids* **2002**, *312−314*, 414–418.
(126) Matsumoto, K.; Hagiwara, R.; Ito, Y.; Kohara, S.; Suzuya, K. *Nucl. Instrum. Methods Phys. Res., Sect. B* **2003**, *199*, 29–33.
(127) Hardacre, C.; Holbrey, J. D.; McMath, S. E. J.; Bowron, D. T.; Soper, A. K. *J. Chem. Phys.* **2003**, *118*, 273.
(128) Hardacre, C.; McMath, S. E. J.; Nieuwenhuyzen, M.; Bowron, D. T.; Soper, A. K. *J. Phys.: Condens. Matter* **2003**, *15*, S159–S166.
(129) Deetlefs, M.; Hardacre, C.; Nieuwenhuyzen, M.; Sheppard, O.; Soper, A. K. *J. Phys. Chem. B* **2005**, *109*, 1593–1598.
(130) Deetlefs, M.; Hardacre, C.; Nieuwenhuyzen, M.; Padua, A. A. H.; Sheppard, O.; Soper, A. K. *J. Phys. Chem. B* **2006**, *110*, 12055–12061.

(131) Hardacre, C.; Holbrey, J. D.; Mullan, C. L.; Nieuwenhuyzen, M.; Youngs, T. G. A.; Bowron, D. T. *J. Phys. Chem. B* **2008**, *112*, 8049–8056.
(132) Hardacre, C.; Holbrey, J. D.; Mullan, C. L.; Nieuwenhuyzen, M.; Youngs, T. G. A.; Bowron, D. T.; Teat, S. J. *Phys. Chem. Chem. Phys.* **2010**, *12*, 1842–1853.
(133) Bowron, D. T.; D'Agostino, C.; Gladden, L. F.; Hardacre, C.; Holbrey, J. D.; Lagunas, M. C.; McGregor, J.; Mantle, M. D.; Mullan, C. L.; Youngs, T. G. A. *J. Phys. Chem. B* **2010**, *114*, 7760–7768.
(134) Hardacre, C.; Holbrey, J. D.; Mullan, C. L.; Youngs, T. G. A.; Bowron, D. T. *J. Chem. Phys.* **2010**, *133*, 074510.
(135) Kanakubo, M.; Umecky, T.; Hiejima, Y.; Aizawa, T.; Nanjo, H.; Kameda, Y. *J. Phys. Chem. B* **2005**, *109*, 13847–13850.
(136) Kanakubo, M.; Aizawa, T.; Nanjo, H.; Kameda, Y.; Amo, Y.; Usuki, T. *Fluid Phase Equilib.* **2010**, *297*, 183–186.
(137) Kanakubo, M.; Ikeda, T.; Aizawa, T.; Nanjo, H.; Kameda, Y.; Amo, Y.; Usuki, T. *Anal. Sci.* **2008**, *24*, 1373–1376.
(138) Katayanagi, H.; Hayashi, S.; Hamaguchi, H.; Nishikawa, K. *Chem. Phys. Lett.* **2004**, *392*, 460–464.
(139) Gontrani, L.; Russina, O.; Lo Celso, F.; Caminiti, R.; Annat, G.; Triolo, A. *J. Phys. Chem. B* **2009**, *113*, 9235–9240.
(140) Bodo, E.; Gontrani, L.; Caminiti, R.; Plechkova, N. V.; Seddon, K. R.; Triolo, A. *J. Phys. Chem. B* **2010**, *114*, 16398–16407.
(141) Macchiagodena, M.; Gontrani, L.; Ramondo, F.; Triolo, A.; Caminiti, R. *J. Chem. Phys.* **2011**, *134*, 114521.
(142) Santos, C. S.; Annapureddy, H. V. R.; Sanjeeva Murthy, N.; Kashyap, H. K.; Castner, E. W., Jr.; Margulis, C. J. *J. Chem. Phys.* **2011**, *134*, 064501.
(143) Santos, C. S.; Sanjeeva Murthy, N.; Baker, G. A.; Castner, E. W., Jr. *J. Chem. Phys.* **2011**, *134*, 121101.
(144) Kashyap, H. K.; Santos, C. S.; Annapureddy, H. V. R.; Sanjeeva Murthy, N.; Margulis, C. J.; Castner, E. W., Jr. *Faraday Discuss.*, **2011** (private communication).
(145) Aoun, B.; Goldbach, A.; Kohara, S.; Wax, J.-F.; González, M. A.; Saboungi, M.-L. *J. Phys. Chem. B* **2010**, *114*, 12623–12628.
(146) Aoun, B.; Goldbach, A.; González, M. A.; Kohara, S.; Price, D. L.; Saboungi, M.-L. *J. Chem. Phys.* **2011**, *134*, 104509.
(147) Qiao, B.; Krekeler, C.; Berger, R.; Delle Site, L.; Holm, C. *J. Phys. Chem. B* **2008**, *112*, 1743–1751.
(148) Ahrland, S.; Chatt, J.; Davis, N. R. *Q. Rev. London* **1958**, *12*, 265.
(149) Pearson, R. G. *J. Am. Chem. Soc.* **1963**, *85*, 3533.
(150) Seki, S.; Hayamizu, K.; Tsuzuki, S.; Fujii, K.; Umebayashi, Y.; Mitsugi, T.; Kobayashi, Y.; Ohno, Y.; Kobayashi, T.; Mita, Y.; Miyashiro, H.; Ishiguro, S. *Phys. Chem. Chem. Phys.* **2009**, *11*, 3509–3514.
(151) Swiderski, K.; McLean, A.; Gordon, C. M.; Vaughan, D. H. *Chem. Commun.* **2004**, 2178.
(152) Lee, S. H.; Lee, S. B. *Chem. Commun.* **2005**, 3469.
(153) Zaitsau, D. H.; Kabo, G. J.; Strechan, A. A.; Paulechka, Y. U.; Tschersich, A.; Verevkin, S. P.; Heintz, A. *J. Phys. Chem. A* **2006**, *110*, 7303.
(154) Armstrong, J. P.; Hurst, C.; Jones, R. G.; Licence, P.; Lovelock, K. R. J.; Satterley, C. J.; Villar-Garcia, I. J. *Phys. Chem. Chem. Phys.* **2007**, *9*, 982.
(155) Santos, L. M. N. B. F.; Lopes, J. N. C.; Coutinho, J. A. P.; Esperanca, J. M. S. S.; Gomes, L. R.; Marrucho, I. M.; Rebelo, L. P. N. *J. Am. Chem. Soc.* **2007**, *129*, 284.
(156) Emel'yanenko, V. N.; Verevkin, S. P.; Heintz, A. *J. Am. Chem. Soc.* **2007**, *129*, 3930–3937.
(157) Luo, H.; Baker, G. A.; Dai, S. *J. Phys. Chem. B* **2008**, *112*, 10077.
(158) Emel'yanenko, V. N.; Verevkin, S. P.; Heintz, A.; Schick, C. *J. Phys. Chem. B* **2008**, *112*, 8095–8098.
(159) Emel'yanenko, V. N.; Verevkin, S. P.; Heintz, A.; Voss, K; Schick, C. *J. Phys. Chem. B* **2009**, *113*, 9871–9876.
(160) Verevkin, S. P. *Angew. Chem., Int. Ed.* **2008**, *47*, 5071–5074.
(161) Emel'yanenko, V. N.; Verevkin, S. P.; Heintz, A.; Corfield, J. A.; Deyko, A.; Lovelock, K. R. J.; Licence, P.; Jones, R. G. *J. Phys. Chem. B* **2008**, *112*, 11734–11742.
(162) Urahata, S. M.; Ribeiro, M. C. C. *J. Chem. Phys.* **2004**, *120*, 1855–1863.
(163) Wang, Y.; Voth, G. A. *J. Am. Chem. Soc.* **2005**, *127*, 12192–12193.
(164) Lopes, J. N. C; Pádua, A. A. H. *J. Phys. Chem. B* **2006**, *110*, 3330–3335.
(165) Hu, Z.; Margulis, C. J. *Proc. Natl. Acad. Sci. U.S.A.* **2006**, *103*, 831–836.
(166) Pádua, A. A. H.; Gomes, M. F. C.; Lopes, J. N. C. *Acc. Chem. Res.* **2007**, *40*, 1087–1096.
(167) Xu, W.; Angell, C. A. *Science* **2003**, *302*, 422–425.
(168) Xu, W.; Cooper, E. I.; Angell, C. A. *J. Phys. Chem. B* **2003**, *107*, 6170.
(169) Yoshizawa, M.; Xu, W.; Angell, C. A. *J. Am. Chem. Soc.* **2003**, *125*, 15411.
(170) Angell, C. A.; Byrne, N.; Belieres, J.-P. *Acc. Chem. Res.* **2007**, *40*, 1228.
(171) Fraser, K. J.; Izgorodina, E. I.; Forsyth, M.; Scott, J. L.; MacFarlane, D. R. *Chem. Commun.* **2007**, 3817.
(172) Schreiner, C.; Zugman, S.; Hartl, R.; Gores, H. J. *J. Chem. Eng. Data* **2010**, *55*, 1784.
(173) Noda, A.; Susan, M. A. B. H.; Kubo, K.; Mitsushima, S.; Hayamizu, K.; Watanabe, M. *J. Phys. Chem. B* **2003**, *107*, 4024.
(174) Tokuda, H.; Hayamizu, K.; Ishii, K.; Susan, M. A. B. H.; Watanabe, M. *J. Phys. Chem. B* **2004**, *108*, 16593.
(175) Tokuda, H.; Hayamizu, K.; Ishii, K.; Susan, M. A. B. H.; Watanabe, M. *J. Phys. Chem. B* **2005**, *109*, 6103.
(176) Tokuda, H.; Ishii, K.; Susan, M. A. B. H.; Tsuzuki, S.; Hayamizu, K.; Watanabe, M. *J. Phys. Chem. B* **2006**, *110*, 2833.
(177) Tokuda, H.; Tsuzuki, S.; Susan, M. A. B. H.; Hayamizu, K.; Watanabe, M. *J. Phys. Chem. B* **2006**, *110*, 19593.
(178) Hayamizu, K.; Tsuzuki, S.; Seki, S.; Umebayashi, Y. *J. Chem. Phys.*, in press.
(179) Nicotera, I.; Oliviero, C.; Henderson, W. A.; Appetecchi, G. B.; Passerini, S. *J. Phys. Chem. B* **2005**, *109*, 22814–22819.
(180) Tsuzuki, S.; Tokuda, H.; Hayamizu, K.; Watanabe, M. *J. Phys. Chem. B* **2005**, *109*, 16474.
(181) Schönert, H. *J. Phys. Chem.* **1984**, *88*, 3359.
(182) Kanakubo, M.; Harris, K. R.; Tsuchihashi, N.; Ibuki, K.; Ueno, M. *J. Phys. Chem. B* **2007**, *111*, 2062.
(183) Kanakubo, M.; Harris, K. R.; Tsuchihashi, N.; Ibuki, K.; Ueno, M. *J. Phys. Chem. B* **2007**, *111*, 13867.
(184) Harris, K. R.; Kanakubo, M.; Tsuchihashi, N.; Ibuki, K.; Ueno, M. *J. Phys. Chem. B* **2008**, *112*, 9830.
(185) Ueno, K.; Imaizumi, S.; Hata, K.; Watanabe, M. *Langmuir* **2009**, *25*, 825.
(186) Sone, K; Fukuda, Y. *Inorganic Thermochromism*; Springer-Verlag: Berlin, Heidelberg, 1987.
(187) Kanzaki, R.; Uchida, K.; Hara, S.; Umebayashi, Y.; Ishiguro, S.; Nomura, S. *Chem. Lett.* **2007**, *36*, 684.
(188) Kanzaki, R.; Uchida, K.; Song, X.; Umebayashi, Y; Ishiguro, S. *Anal. Sci.* **2008**, *24*, 1347–1350.
(189) Kanzaki, R.; Song, X.; Umebayashi, Y.; Ishiguro, S. *Chem. Lett.* **2010**, *39*, 578–579.
(190) Ishiguro, S; Umebayashi, Y.; Kanzaki, R.; Fujii, K. *Pure Appl. Chem.* **2010**, *82*, 1927–1941.
(191) Koppel, I. A.; Taft, R. W.; Anvia, F.; Zhu, S. Z.; Hu, L. Q.; Sung, K. S.; Desmarteau, D. D.; Yagupolskii, L. M. *J. Am. Chem. Soc.* **1994**, *116*, 3047.
(192) Leito, I.; Raamat, E.; Kütt, A.; Saame, J.; Kipper, K.; Koppel, I. A.; Koppel, I.; Zhang, M.; Mishima, M.; Yagupolskii, L. M.; Garlyauskayte, R. Yu.; Filatov, A. A. *J. Phys. Chem. A* **2009**, *113*, 8421–8424.
(193) Gejji, P.; Johansson, P.; Tegenfeldt, J.; Lindgren, J. *Comput. Polym. Sci.* **1995**, *5*, 99.
(194) Johansson, P.; Grondin, J.; Lassègues, J.-C. *J. Phys. Chem. A* **2010**, *114*, 10700–10705.
(195) Tamura, T.; Yoshida, K.; Hachida, T.; Tsuchiya, M.; Nakamura, M.; Kazue, Y.; Tachikawa, N.; Dokko, K.; Watanabe, M. *Chem. Lett.* **2010**, *39*, 753–755.

(196) Tamura, T.; Hachida, T.; Yoshida, K.; Tachikawa, N.; Dokko, K.; Watanabe, M. *J. Power Sources* **2010**, *195*, 6095–6100.
(197) Amari, T.; Funahashi, S.; Tanaka, M. *Inorg. Chem.* **1988**, *27*, 3368–3372.
(198) Soyama, S.; Ishii, M.; Funahashi, S.; Tanaka, M. *Inorg. Chem.* **1992**, *31*, 536–538.
(199) Inada, Y.; Ozutsumi, K.; Funahashi, S.; Soyama, S.; Kawashima, T.; Tanaka, M. *Inorg. Chem.* **1993**, *32*, 3010–3014.